Engineered Science
DOI: https://dx.doi.org/10.30919/es1173

Optimized Performance of Closed Loop Control Electromagnetic Field for the Electric Generators with Energy Storage

Ponthep Vengsungnle[1], Sahassawas Poojeera,[2] Apichat Srichat,[3] and Paisarn Naphon[4,*]

Abstract

The effects of the generated electromagnetic field on the operation of electrical generators with energy storage have been investigated. A prototype comprises an electromagnetic field system, an electrical generator, and an energy conversion and storage system. The electromagnetic generator field comprises both the rotor and the stator. Two rotors are made from an aluminum block with 64 holes for 128 Neodymium magnets. The aluminum block makes eight stator coils with 325 turns of copper wire. The testing method was repeated for various electromagnetic field sources, beginning motor driving time, and generator types for the best performance. The highest spinning speed of the rotor is determined to be about 1920 rpm for the G-2, 1720 rpm for the G-3, and 940 rpm for the G-1. Acquiring a satisfactory beginning motor driving time of 5 seconds is possible. The maximum performance is achieved by the G-2 generator, which has four electromagnetic field sources and an initial motor driving time of 5 seconds. However, the generator has been continually enhanced to achieve greater performance, including system adaptability, connection and drive system, and load and energy storage system.

Keywords: Optimized performance; Energy storage; Electromagnetic field; Generator.
Received: 13 January 2024; Revised: 24 May 2024; Accepted: 31 May 2024.
Article type: Research article.

1. Introduction

Energy consumption has increased recently, resulting in higher energy costs and adverse environmental impacts. Therefore, power generation systems have been continuously developed using various technologies. Turbines can generate more energy in tight spaces than other energy sources, even though wind turbines are developed on a small scale with new technologies for commercial purposes. Many scientists have developed generators. For example, Popa and Lucjorat[1] developed an electrical generator coupled to the vertical motion of ocean waves. Ishikawa *et al*.[2] investigated the pulsed generator. Moradi and Afjei[3] researched and experimentally analyzed the magnetic field of a brushless direct current generator. Ting and Yeh[4] studied an individual wind generator, and Wang *et al*.[5] considered the hybrid continuous magnetic generator. Next, Rao *et al*.[6] designed linear generators for permanently energized magnets. The works presented an induced generator with a vertical twin-rotor, as reported by[7,8,11]. Homadi and Hall[9] studied the low-temperature magnetic generator. Next, Salek *et al*.[10] studied the hydroxy generator's improved thermal performance. Shao *et al*.[12] investigated using a triboelectric nanogenerator and electromagnetic generator to harvest energy as a convenient source. Vivekananthan *et al*.[13] reported that the triboelectric electromagnetic hybrid generator derived from the magnetic particles Fe_2O_3 is used for seismic detection without energy consumption. Li *et al*.[14] designed an electromagnetic spherical movement generator with a multi-layered structure. Li *et al*.[15] have developed a new flexible TEHG based on magnetized micro-pins for human motion monitoring.

[1] *Department of Agricultural Machinery Engineering, Faculty of Engineering and Architecture, Rajamangala University of Technology Isan, Nakhonratchasima 30000, Thailand.*
[2] *Department of Mechanical Engineering, Faculty of Engineering, Rajamangala University of Technology Isan, Khon Kaen Campus, 40000, Thailand.*
[3] *Department of Mechanical Engineering, Faculty of Technology, Udon Thani Rajabhat, University, 41000, Thailand.*
[4] *Thermo-Fluids and Heat Transfer Enhancement Research Lab. (TFHT), Department of Mechanical Engineering, Faculty of Engineering, Srinakharinwirot University, 63 Rangsit-Nakhornnayok Rd., Ongkharak, Nakhorn-Nayok, 26120, Thailand.*
**Email:* paisarnn@g.swu.ac.th (P. Naphon)

The method of self-assembly by magnetic field-induced spraying with an electro-magnetization technique was first proposed for the cost-effective manufacture of magnetized microneedles for TEHG. Xu *et al*.[16] applied the efficiency of converting torque and energy between the rotating triboelectric nanogenerator and the electromagnetic generator. EMG's energy conversion efficiency increases as the mechanical input power increases, while TENG's energy conversion efficiency remains almost constant. Han *et al*.[17] investigated the triboelectric-electromagnetic hybrid generator. The results demonstrated that the ESMF provides good products for applications. Wu *et al*.[18] improved the energy conversion efficiency of the hybrid electrostatic-electromagnetic generator. Zhang *et al*.[19] introduced a three-cylinder hybrid generator (a triboelectric nanogenerator and an electromagnetic generator). Dang *et al*.[20] suggested a triboelectric-electromagnetic hybrid generator based on the inertial conversion mechanism. As the wind velocity increases, the centrifugally-controlled inertia conversion mechanism drives triboelectric nanogenerator units. Li *et al*.[21] studied the effect of magnet arrangement on output performance with three cases: an alternative magnetic scheme, a Halbach scheme, and a separate scheme. Hu *et al*.[22] investigated triboelectric and electromagnetic nanogenerators. Zhang *et al*.[23] suggested a new vibro-electrodielectric impact hybrid generator. Bhatta *et al*.[24] investigated two-mode, magnetically-assisted triboelectric sensors embedded in an electromagnetic generator. Cho *et al*.[25] suggested a hybrid hydraulic wheel generator with a triboelectric disk nanogenerator and an electromagnetic generator as an energy source. Vidal *et al*.[26] investigated electromagnetic generators, suitable contenders for powering small-scale and large-scale devices. Zhu *et al*.[27] investigated the triboelectric-electromagnetic generator with aerodynamic improvement for the energy collection of the breeze. Carneiro *et al*.[28] optimized the electromagnetic generator's efficiency by auto-adapting the structure. Sharghi and Bilgen[29] studied the collection of energy from a pendular system with an electromagnetic generator. Moradian *et al*.[30] developed a pendular spherical electromagnetic generator. Xu *et al*.[31] examined the effect of the wind on the performance of permanent magnetic wind turbines with dual three-phase winding. The results showed that the magnet windmill with double 3-phase winding could achieve maximum power. Savsteenko *et al*.[32] proposed the vehicle starter-generator with a differential electric drive. The design and optimization of a starter generator with a differential electric drive based on a direct current (DC) electric motor are completed. Milev *et al*.[33] concentrated only on the design phases of a ship-based electric power station with self-excited brushless synchronous generators. Kumar *et al*.[34] created a solar-powered battery and diesel generator for an electric car charging station utilizing a hybrid intelligent controller with ANN. Amuhaya *et al*.[35] investigated permanent magnet synchronous generator topologies with rotor field coils to achieve low mass with high efficiency in smart grids. Permanent magnets are surface-mounted on conventional double-excited synchronous generators. Ullah *et al*.[36] presented a new magnet-less dual electrical and dual mechanical port wound field-excited flux switching generator for direct-drive counter-rotating wind turbines magnet-less dual electrical and dual mechanical port wound field-excited flux switching generator. Hu *et al*.[37] proposed organic phase change materials for energy storage materials with the ability to store and release thermal energy at a constant temperature. As noted in the preceding review, most previous research proposed and designed the generators using different power sources.

Electric generator designs and applied electromagnetic fields are still limited, especially in hybrid energy source systems with closed-loop control systems. Previous research[38] experimentally investigated the suggested prototype of a rotating magnetic field driven by an electromagnetic field.

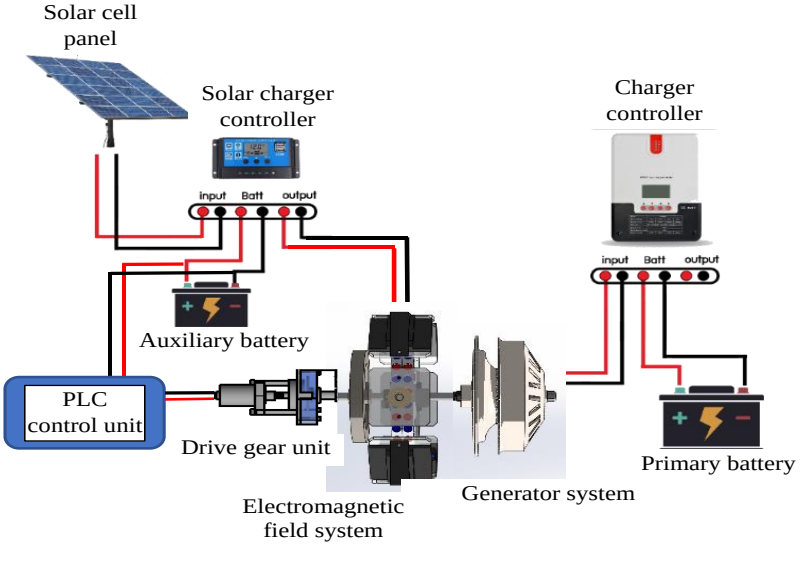

Fig. 1 Diagram of the two transmission systems from solar energy to electric energy.

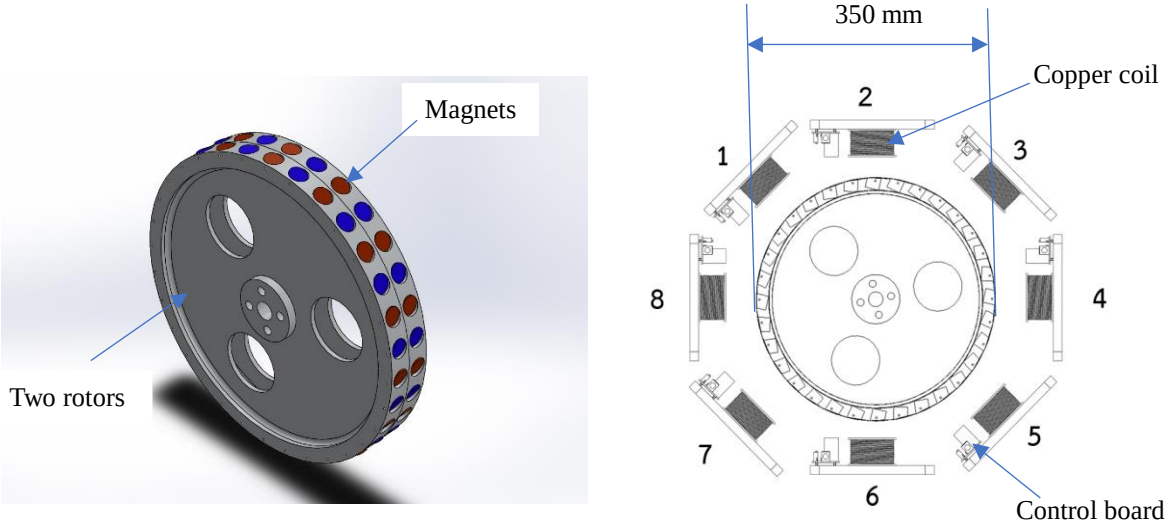

Fig. 2 Diagram of two rotors and stator antenna unit.

However, the system was improved to obtain greater performance. As a result, the present work stems from the research[38] in which the newly developed electromagnetic generator with an additional solar cell unit aided the initial motor start unit. All systems are adjustable in the procedure, and the operational condition has been done utilizing programmable logic controller (PLC). The effects of the initial motor start time, number of copper coils, and generator types (directly powered by the main shaft) have been investigated to obtain the performance.

2. Experimental facilities and procedure

2.1 Experimental facilities

As shown in Fig. 1, the experimental system consists of an electromagnetic field system, a generator set with a controller loader system, a solar cell system, and a motor start system. This system has two battery units for easy working control-the first lithium-ion auxiliary battery (12V) for the motor's first start. The energy of this unit is obtained from the solar cell system. The second one (24V) is the primary battery unit, where the power delivered from the electromagnetic generator is stored in a primary battery. In contrast, some energy from this battery is used to feed the electromagnetic field system, the PLC, and is supplied to electrical devices.

However, the system can be designed with a single battery unit. The electromagnetic field system consists of a rotor and a stator antenna. Two 350 mm diameter and 25mm thick rotors are made from an aluminum block with 64 positions for 128 NeFeB magnets, as shown in Fig. 2. As illustrated in Figs. 2 and 3, the stator antenna unit with eight copper coils (24 V) is manufactured from an aluminum block with copper wire installed on the circular aluminum frame approximately 5 mm from the rotor unit. As illustrated in Fig. 4, the electrical generator with controller charger system consists of a generator (400W), MPPT controller charger system (24V), main lithium-ion battery (320Ah, 24V), and DC-AC inverter(24V). The solar cell system includes a solar cell panel, a solar charger controller, and a lithium-ion auxiliary battery (12V) for the motor's first start. Between the rotor and the initial starting unit, an inertia wheel (with drive gear unit) 350

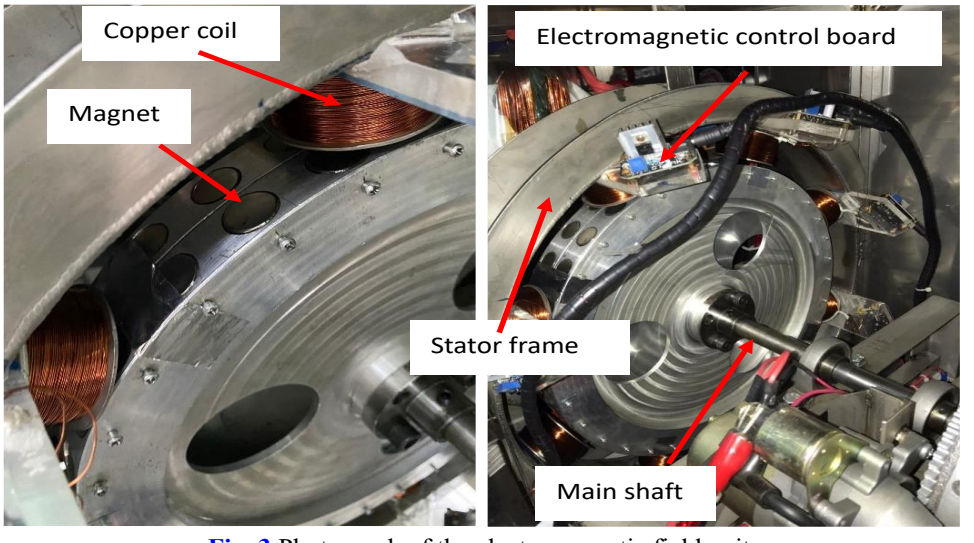

Fig. 3 Photograph of the electromagnetic field unit.

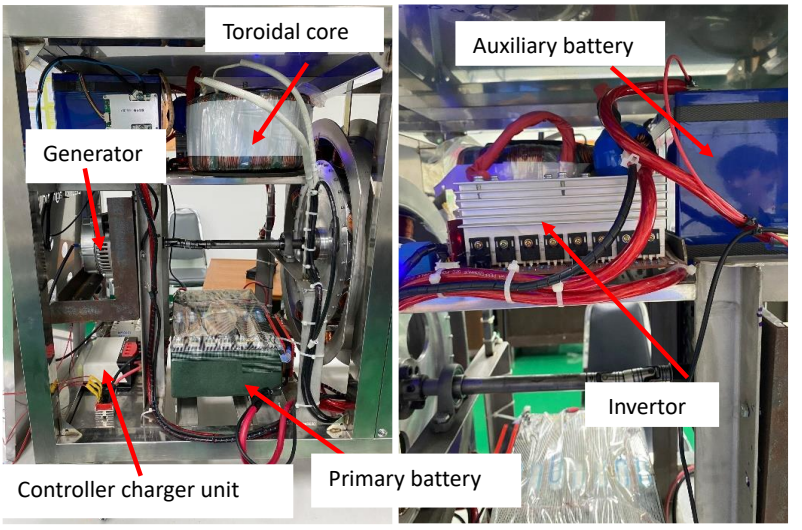

Fig. 4 Photograph of the inverter unit, generator unit, and controller charger unit.

mm in diameter is installed on the main shaft (30 mm in diameter), with the other end immediately attached to the generator shaft via a connection. As illustrated in Fig. 5, starting the DC motor (12V) is only utilized for the initial revolution of the rotor, which the programmable controller controls.

2.2 Experimental test method

First, the system is powered by energizing the switching power and the energy of the primary battery module, which includes eight stator copper coils. The motor contacts the driving gear to power the main shaft (rotor and generator), which the PLC controls. The initial gear motor then travels away from the driving gear and de-energizes, and the electromagnetic field of each stator reel dips the rotor. A tachometer is used to measure the rotation rate of the rotor. Eight antennas operate independently and may be controlled by a PLC, as illustrated in Fig. 6. Each antenna consists of a copper coil, electromagnetic control board, power supply unit, light bulb monitoring system, and a PLC control system. As seen in Fig. 2, each antenna station functions independently. The digital circuit control may change the electromagnetic unit (eight antennas) and the connecting/disconnecting times. This is shown by the operation of each antenna's light bulbs, which flash synchronously. To determine the impact of the starting motor drive time, the electromagnetic field unit (copper coils), and operation time, relevant parameters may be adjusted, and each antenna may be switched on/off by pressing its symbol on the display.

The experimental processes have been performed with three different generators, as shown in Fig. 7. The Gen-1 is modified from the inverter direct drive motor of the washing machine, Gen-2 is modified from the car alternator, and Gen-3 is a low-speed generator. The primary battery provides the power for the system. The generator's output is stored in the primary battery, monitored, and measured using a digital AC/DC clamp meter. The system is also intended to provide some of the power for the solar cell system. Table 1 shows the uncertainty and precision of the instruments.

3. Results and discussion

The power delivered comes from the electromagnetic

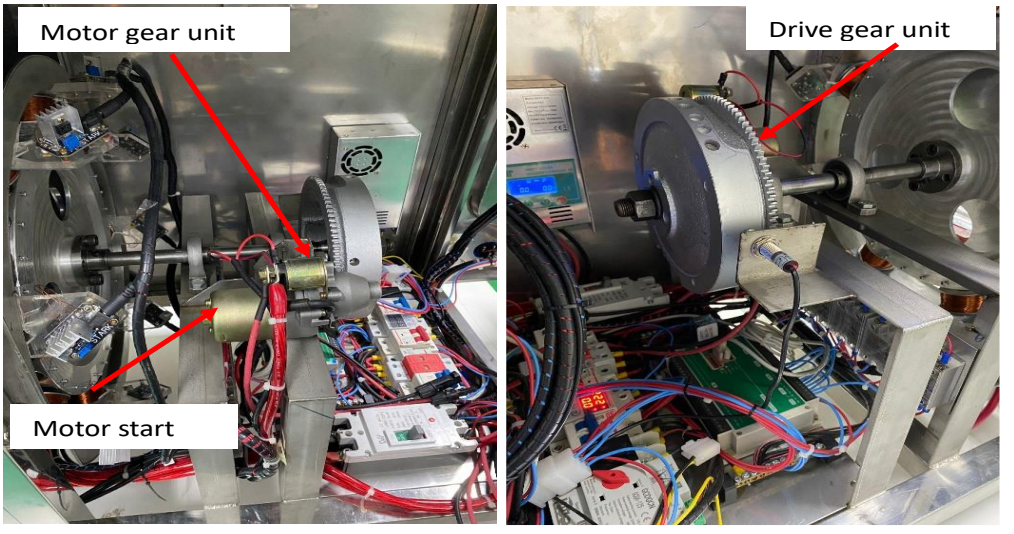

Fig. 5 Photograph of the motor start unit.

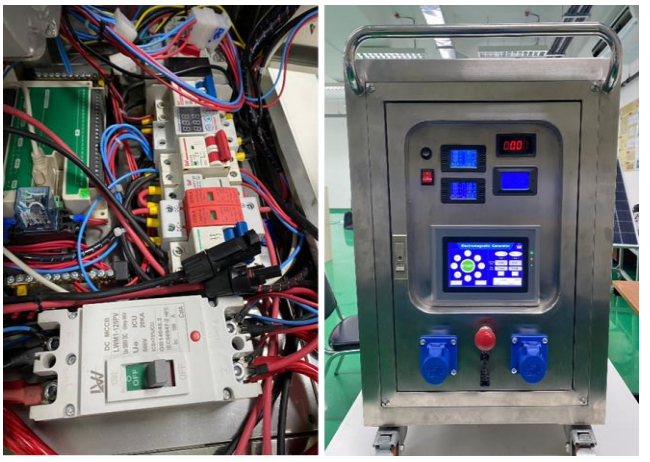

Fig. 6 Photograph of the electric control system and control panel.

Table 1. Uncertainty and accuracy of the instruments.

Instrument	Accuracy (%)	Uncertainly
Power supply, V	0.2	±0.5
Multi-meter	0.1	±0.05
Tachometer	0.05	±0.1

generator, which is stored in a main battery. The energy of the auxiliary battery is obtained from the solar cell system, in which the maximum solar energy occurs at noon. In contrast, the lowest occurs in the morning and evening.[38] The system's operating conditions can be monitored and controlled using a PLC system with a touchscreen. This study examines various electromagnetic field sources, three generators (Fig. 7), and initial motor drive time.

Figure 8 shows the rotor speed variation with the electromagnetic field sources (EFSs) with three generators for the initial motor drive time of 10 s. The main rotor shaft is directly connected to the generator shaft with the connecting device. The number of EFSs used in the present study is 3-8. For three generators, the speed increases with the number of EFSs. Gen-1 begins to rotate when the number of EFSs exceeds 4, and the rotor speed increases with increasing the number of EFSs. Gen-2 provides a higher rotor rpm for all the number of EFS than Gen-3 and Gen-1, giving a maximum speed of 1920 rpm for the EFSs of eight, 1700 rpm for Gen-3, and 950 rpm for Gen-1. Therefore, all the experimental conditions were carried out with the Gen-2 for different relevant parameters for the operating time of 30 minutes.

Figure 9 illustrates the effect of the initial motor drive time on the rotor speed for Gen-2 with EFSs = 6. In the first stage, the gear motor comes into contact with the drive gear to drive the main shaft (rotor and alternator). After that, the gear motor moves away from the drive gear and enters power-off mode, which PLC controls. The figure illustrates that the rotor speed increases as the initial motor drive time increases. In addition, it is found that the maximum rotor speed at the initial motor drive time of 5 s is equal to the initial motor drive time of 10 s (Fig. 8). Therefore, to get the maximum rotor speed and save energy consumption of the initial motor start, take 5 s the initial motor drive time is suitable.

Figures. 10 and 11 show the variations of the charged and consumed energy (voltage level) for a 30-minute running time. The stored electric energy is generated from the generator, which is charged in the primary battery unit. At the same time, some power from the primary battery is supplied for the whole system, including the control system and electromagnetic field system. The charged and supplied electric energy (voltage level) increase with the initial motor drive time (IMDT) increase. Fig. 12 shows the net electric energy with an initial motor drive time (IMDT) for EFSs = 6. It can be found that the charged energy (voltage level) rate is higher than the discharged energy (voltage level) rate by around 10.99% for an initial motor drive time of 2 s and 18.18% for an initial

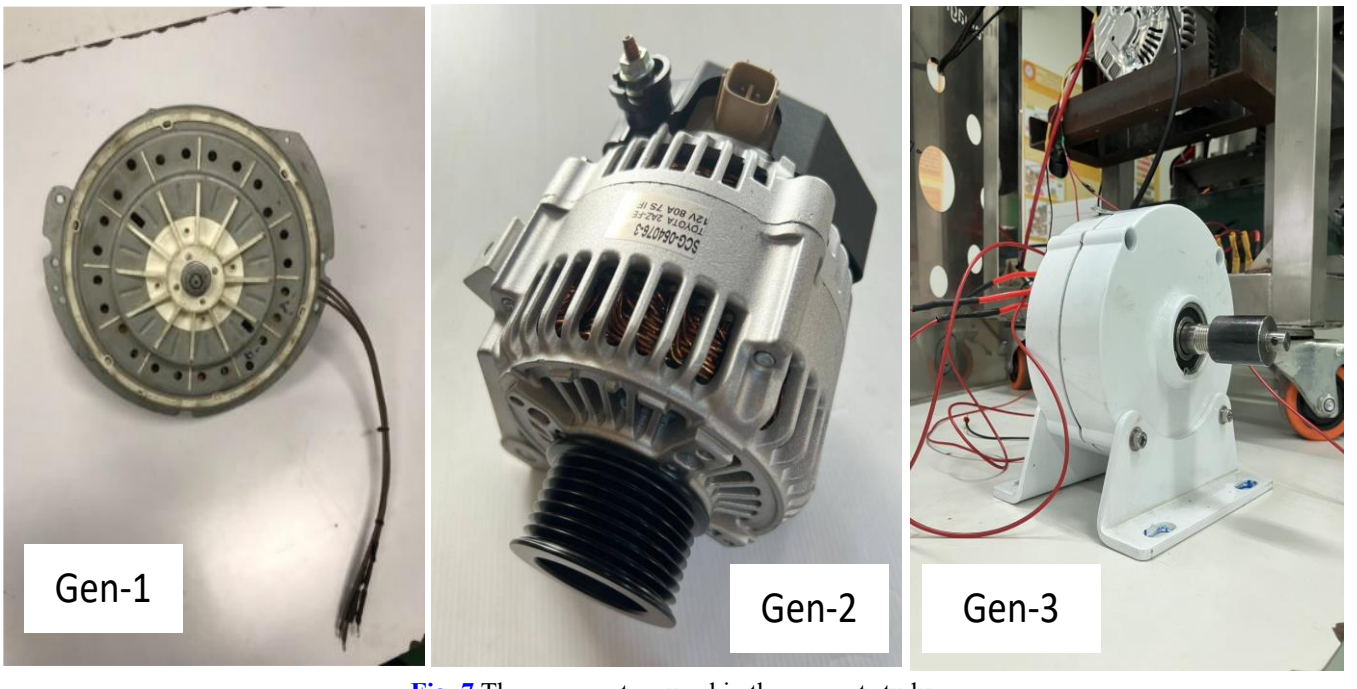

Fig. 7 Three generators used in the present study.

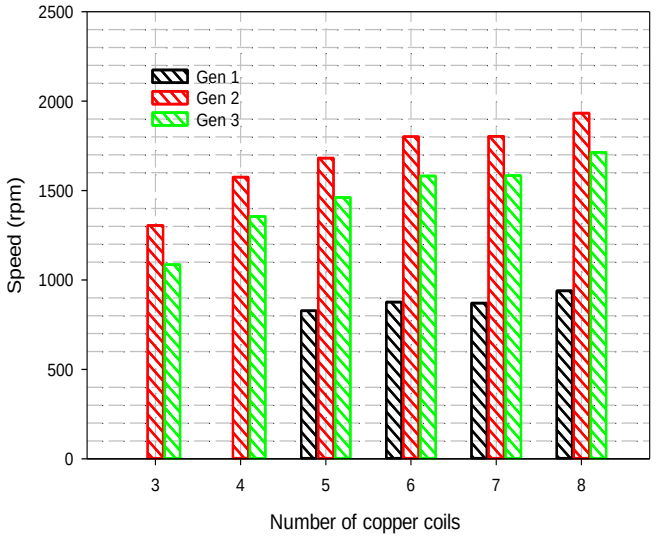

Fig. 8 Variations of rotor speed with the number of EFSs for different generators.

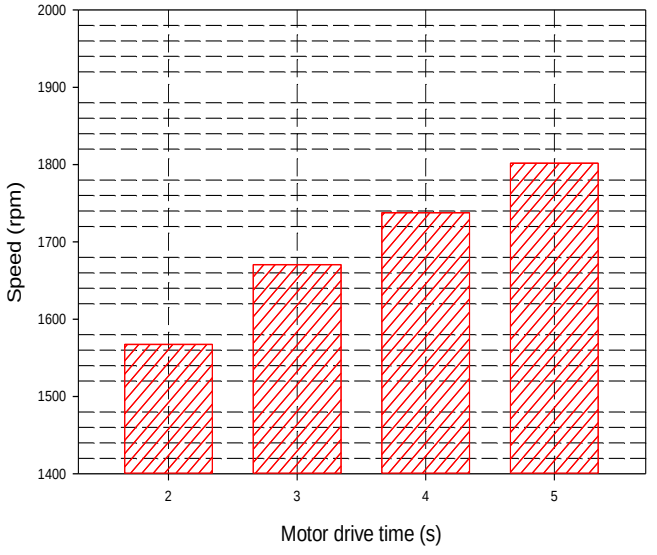

Fig. 9 Variation of rotor speed with initial motor drive time (IMDT) for EFSs = 6, operating time = 30 minutes.

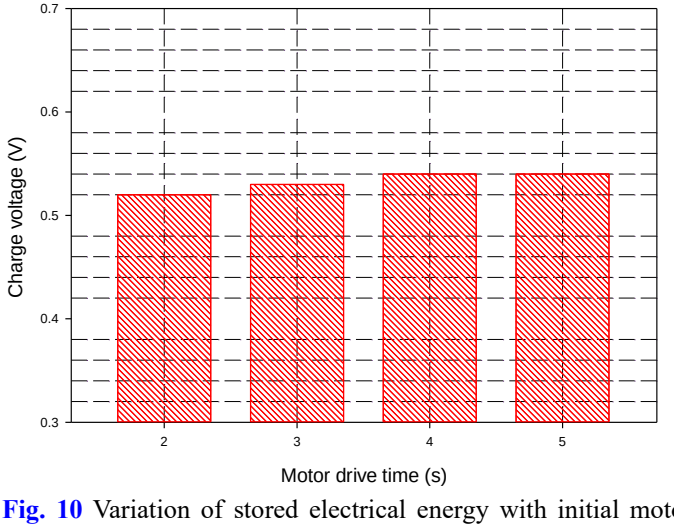

Fig. 10 Variation of stored electrical energy with initial motor drive time (IMDT) for EFSs = 6, operating time = 30 minutes.

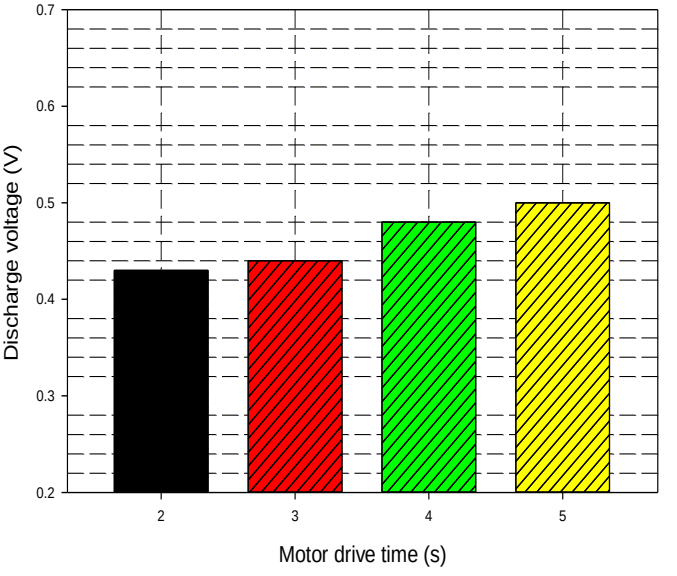

Fig. 11 Variation of used electrical energy with initial motor drive time (IMDT) for EFSs = 6, operating time = 30 minutes.

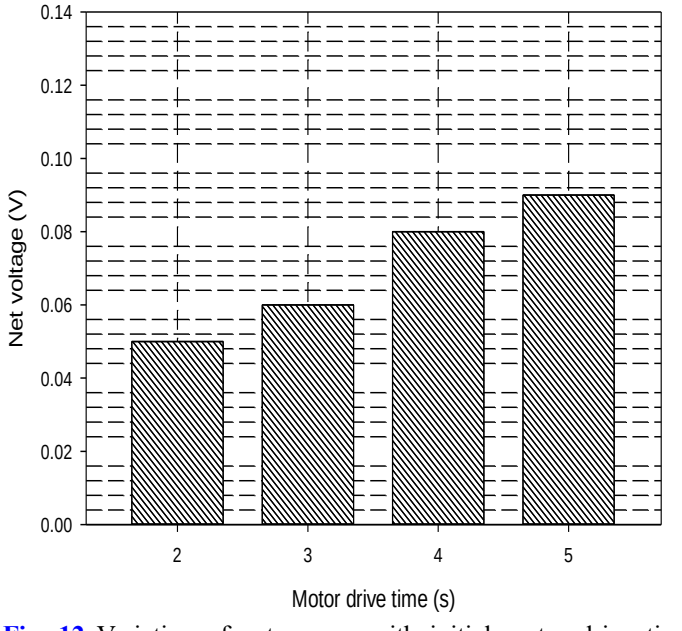

Fig. 12 Variation of net energy with initial motor drive time (IMDT) for EFSs = 6, operating time = 30 minutes.

motor drive time of 5 s.

The results above show that the proper initial drive motor time (IMDT) of 5 s is used in the following experiment. The effect of the electromagnetic field sources (EFSs) on the rotor speed using a 5 s IMDT for 30 minutes is shown in Fig. 13. The strength of the electromagnetic field varies according to the source. As a result, higher electromagnetic field sources (EFSs) increase rotor speed, resulting in a higher energy charged rate. As shown in Fig. 14, the primary battery's maximum and minimum energy charged rates are 0.91 V and 0.44 V for the EFSs of 8 and 3, respectively. Generally, the battery charging rate depends on the voltage remaining in the battery and the feed current level. For a given feed current level (1.1-1.2A), the empty battery or low voltage remaining

level, the battery charging rate is also high, and the charged rate decreases as the battery is close to full level. In the present experiment, the remaining voltage level of the battery for each condition is not the same level, which results in the battery charging rate. From the results from Fig. 14, the remaining voltage level of the battery for EFSs of 4 is lower than EFSs of 5 and 6. Therefore, the EFSs of 4 give a higher charging rate than the EFSs of 5 and 6. However, the energy consumption increases with increasing EFSs, as shown in Fig. 15. The variation of the net energy level with different EFSs for an operating time of 30 minutes, as shown in Fig. 16. It can be found that the charging rates are higher than the discharging rate for EFSs of 3, 4, 5, 6, 7. However, for EFS of 8, the discharging rate is higher than the charging rate. The present study, the system performance is the ratio of net voltage to charge voltage ((Charge voltage-discharge voltage)/Charge voltage) of 56.56%, 73.08%, 20.14%, 4.31%, 20.61%, and -3.46% for EFSs 3, 4, 5, 6, 7, and 8, respectively.

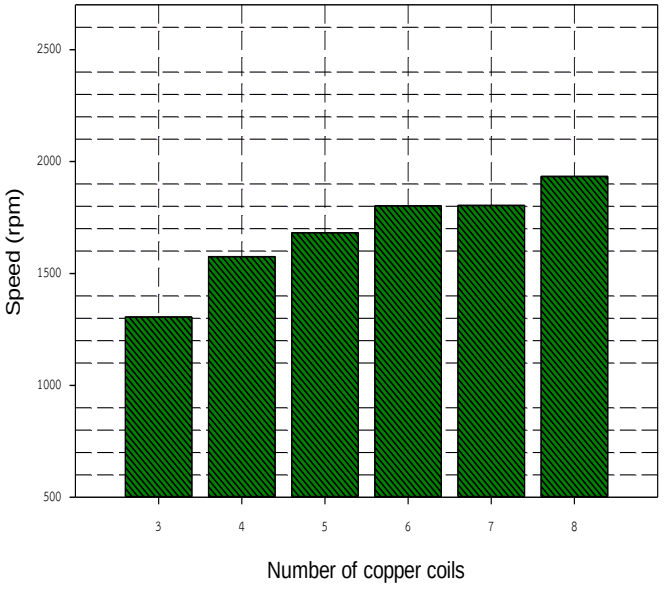

Fig. 13 Variation of rotor speed with EFSs for IMDT = 5 s, operating time = 30 minutes.

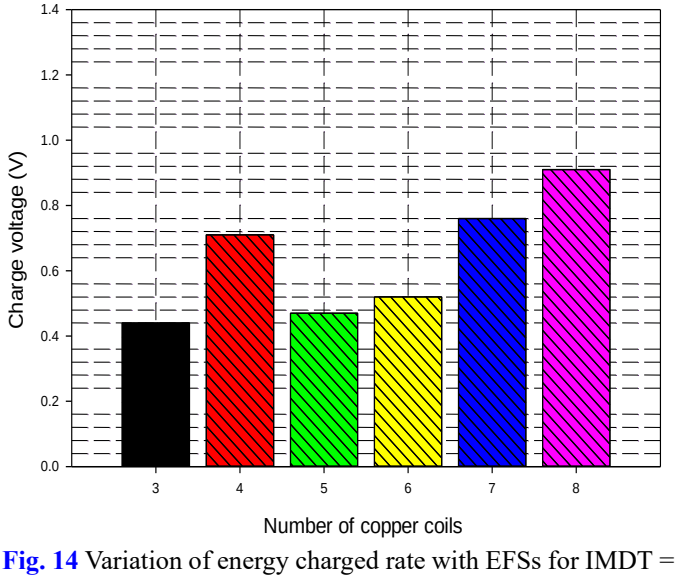

Fig. 14 Variation of energy charged rate with EFSs for IMDT = 5 s, operating time = 30 minutes.

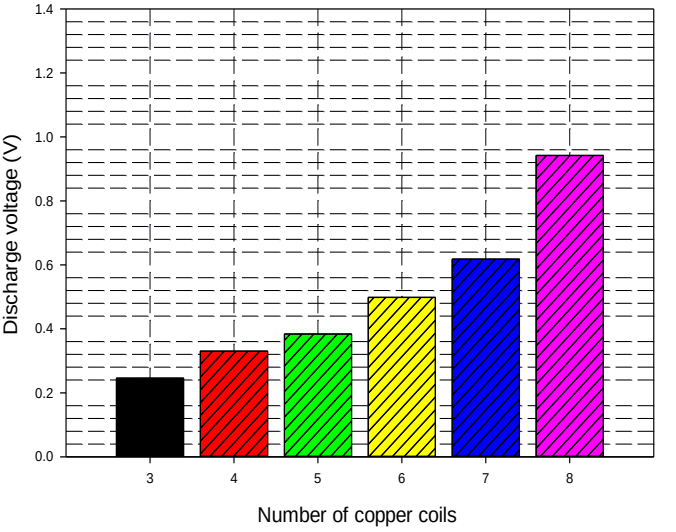

Fig. 15 Variation of energy consumption with EFSs for IMDT = 5 s, operating time = 30 minutes.

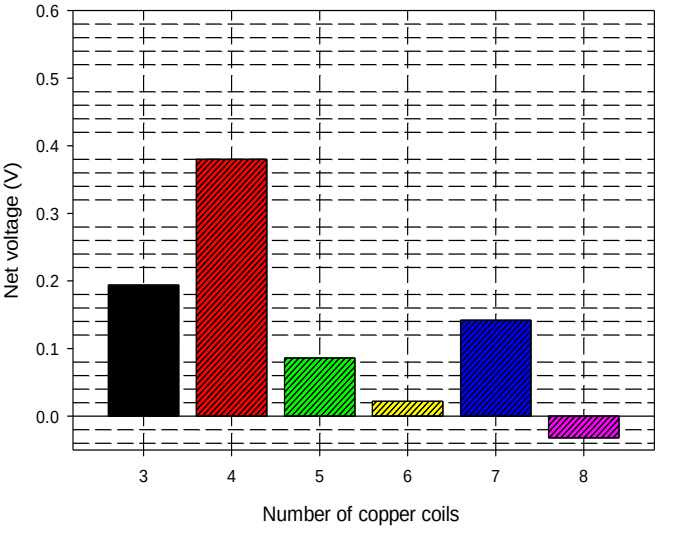

Fig. 16 Variation of net energy with EFSs for IMDT = 5 s, operating time = 30 minutes.

4. Conclusions

A new electromagnetic field system with an initial motor drive and solar cell system for the auxiliary energy storage system, monitored and controlled with a PLC system, has been designed. The optimum state for an electromagnetic field generator was examined. The effects of the initial motor drive time, generator types, and electromagnetic field sources on system performance were considered. It is noted that the suitable electromagnetic field generator with a G-2 generator, four EFSs, and IMDT of 5 s gives the highest performance. The maximum speed and performance are around 1920 revolutions per minute and 73.05%, respectively. However, some relevant parameters on the performance must be continuously performed. After the optimized conditions, some control systems can be removed from the system to reduce energy consumption and operate with the solar cell system that

feeds the system, which results in higher efficiency, a simplified system, and easier operation control.

Acknowledgments

The authors would like to express their appreciation for the financial support of the Faculty of Engineering at the University of Srinakharinwirot (SWU).

Conflict of Interest

There is no conflict of interest.

Supporting Information

Not applicable.

References

[1] N. Călin Popa, A. Siblini, L. Jorat, Gravitational electrical generator on magnetic fluid cushion, *Journal of Magnetism and Magnetic Materials*, 1999, **201**, 407-409, doi: 10.1016/s0304-8853(99)00092-x.

[2] M. Ishikawa, Y. Koshiba, T. Matsushita, Effects of induced magnetic field on large scale pulsed MHD generator with two phase flow, *Energy Conversion and Management*, 2004, **45**, 707-724, doi: 10.1016/s0196-8904(03)00182-1.

[3] H. Moradi, E. Afjei, Analysis of brushless DC generator incorporating an axial field coil, *Energy Conversion and Management*, 2011, **52**, 2712-2723, doi: 10.1016/j.enconman.2011.01.027.

[4] C.-C. Ting, L.-Y. Yeh, Developing the full-field wind electric generator, *International Journal of Electrical Power & Energy Systems*, 2014, **55**, 420-428, doi: 10.1016/j.ijepes.2013.09.030.

[5] H. Wang, Z. Qu, S. Tang, M. Pang, M. Zhang, Analysis and optimization of hybrid excitation permanent magnet synchronous generator for stand-alone power system, *Journal of Magnetism and Magnetic Materials*, 2017, **436**, 117-125, doi: 10.1016/j.jmmm.2017.04.035.

[6] K. S. R. Rao, T. Sunderan, M. R. Adiris, Performance and design optimization of two model based wave energy permanent magnet linear generators, *Renewable Energy*, 2017, **101**, 196-203, doi: 10.1016/j.renene.2016.07.019.

[7] H. Torkaman, A. Keyhani, A review of design consideration for Doubly Fed Induction Generator based wind energy system, *Electric Power Systems Research*, 2018, **160**, 128-141, doi: 10.1016/j.epsr.2018.02.012.

[8] D.-Y. Tsai, H.-Y. Hsu, G.-E. Chen, C.-C. Ting, Developing the full-field wind generator integrated with the vertical twin rotors, *International Journal of Electrical Power & Energy Systems*, 2018, **103**, 395-403, doi: 10.1016/j.ijepes.2018.06.003.

[9] A. Homadi, T. Hall, Investigation study of modeling a new oscillating generator utilizing low temperature, magnetic susceptibility and waste heat, *Thermal Science and Engineering Progress*, 2019, **9**, 162-168, doi: 10.1016/j.tsep.2018.11.012.

[10] F. Salek, M. Zamen, S. V. Hosseini, Experimental study, energy assessment and improvement of hydroxy generator coupled with a gasoline engine, *Energy Reports*, 2020, **6**, 146-156, doi: 10.1016/j.egyr.2019.12.009.

[11] M. Mansour, M. N. Mansouri, S. Bendoukha, M. F. Mimouni, A grid-connected variable-speed wind generator driving a fuzzy-controlled PMSG and associated to a flywheel energy storage system, *Electric Power Systems Research*, 2020, **180**, 106137, doi: 10.1016/j.epsr.2019.106137.

[12] H. Shao, Z. Wen, P. Cheng, N. Sun, Q. Shen, C. Zhou, M. Peng, Y. Yang, X. Xie, X. Sun, Multifunctional power unit by hybridizing contact-separate triboelectric nanogenerator, electromagnetic generator and solar cell for harvesting blue energy, *Nano Energy*, 2017, **39**, 608-615, doi: 10.1016/j.nanoen.2017.07.045.

[13] V. Vivekananthan, A. Chandrasekhar, N. R. Alluri, Y. Purusothaman, G. Khandelwal, R. Pandey, S.-J. Kim, Fe_2O_3 magnetic particles derived triboelectric-electromagnetic hybrid generator for zero-power consuming seismic detection, *Nano Energy*, 2019, **64**, 103926, doi: 10.1016/j.nanoen.2019.103926.

[14] X. Li, J. Liu, W. Chen, S. Bai, Analytical magnetics and torque modeling of a multi-layer electromagnetic driven spherical motion generator, *Journal of Magnetism and Magnetic Materials*, 2020, **493**, 165707, doi: 10.1016/j.jmmm.2019.165707.

[15] Y. Li, Z. Chen, G. Zheng, W. Zhong, L. Jiang, Y. Yang, L. Jiang, Y. Chen, C.-P. Wong, A magnetized microneedle-array based flexible triboelectric-electromagnetic hybrid generator for human motion monitoring, *Nano Energy*, 2020, **69**, 104415, doi: 10.1016/j.nanoen.2019.104415.

[16] S. Xu, X. Fu, G. Liu, T. Tong, T. Bu, Z. L. Wang, C. Zhang, Comparison of applied torque and energy conversion efficiency between rotational triboelectric nanogenerator and electromagnetic generator, *Science*, 2021, **24**, 102318, doi: 10.1016/j.isci.2021.102318.

[17] Q. Han, Z. Ding, W. Sun, X. Xu, F. Chu, Hybrid triboelectric-electromagnetic generator for self-powered wind speed and direction detection, *Sustainable Energy Technologies and Assessments*, 2020, **39**, 100717, doi: 10.1016/j.seta.2020.100717.

[18] Z. Wu, Z. Cao, R. Ding, S. Wang, Y. Chu, X. Ye, An electrostatic-electromagnetic hybrid generator with largely enhanced energy conversion efficiency, *Nano Energy*, 2021, **89**, 106425, doi: 10.1016/j.nanoen.2021.106425.

[19] Q. Zhang, L. Li, T. Wang, Y. Jiang, Y. Tian, T. Jin, T. Yue, C. Lee, Self-sustainable flow-velocity detection via electromagnetic/triboelectric hybrid generator aiming at IoT-based environment monitoring, *Nano Energy*, 2021, **90**, 106501, doi: 10.1016/j.nanoen.2021.106501.

[20] H. Dang, Y. Wang, S. Zhang, Q. Gao, X. Li, L. Wan, Z. L. Wang, T. Cheng, Triboelectric-electromagnetic hybrid generator with the inertia-driven conversion mechanism for wind energy harvesting and scale warning, *Materials Today Energy*, 2022, **29**, 101136, doi: 10.1016/j.mtener.2022.101136.

[21] Z. Li, X. Jiang, W. Xu, Y. Gong, Y. Peng, S. Zhong, S.

Xie, Performance comparison of electromagnetic generators based on different circular magnet arrangements, *Energy*, 2022, **258**, 124759, doi: 10.1016/j.energy.2022.124759.
[22] C. Hu, Y. Yang, Z. L. Wang, Quantitative comparison between the effective energy utilization efficiency of triboelectric nanogenerator and electromagnetic generator post power management, *Nano Energy*, 2022, **103**, 107760, doi: 10.1016/j.nanoen.2022.107760.
[23] C. Zhang, J. Xu, S. Fang, Z. Qiao, D. Yurchenko, Z. Lai, A pendulum-based absorber-harvester with an embedded hybrid vibro-impact electromagnetic-dielectric generator, *Nano Energy*, 2023, **107**, 108126, doi: 10.1016/j.nanoen.2022.108126.
[24] T. Bhatta, G. B. Pradhan, K. Shrestha, S. Lee, S. S. Rana, S. Sharma, H. Song, S. Jeong, J. Y. Park, Magnets-assisted dual-mode triboelectric sensors integrated with an electromagnetic generator for self-sustainable wireless motion monitoring systems, *Nano Energy*, 2022, **103**, 107860, doi: 10.1016/j.nanoen.2022.107860.
[25] H. Cho, I. Kim, J. Park, D. Kim, A waterwheel hybrid generator with disk triboelectric nanogenerator and electromagnetic generator as a power source for an electrocoagulation system, *Nano Energy*, 2022, **95**, 107048, doi: 10.1016/j.nanoen.2022.107048.
[26] J. V. Vidal, P. Rolo, P. M. R. Carneiro, I. Peres, A. L. Kholkin, M. P. Soares dos Santos, Automated electromagnetic generator with self-adaptive structure by coil switching, *Applied Energy*, 2022, **325**, 119802, doi: 10.1016/j.apenergy.2022.119802.
[27] M. Zhu, J. Zhang, Z. Wang, X. Yu, Y. Zhang, J. Zhu, Z. L. Wang, T. Cheng, Double-blade structured triboelectric–electromagnetic hybrid generator with aerodynamic enhancement for breeze energy harvesting, *Applied Energy*, 2022, **326**, 119970, doi: 10.1016/j.apenergy.2022.119970.
[28] P. M. R. Carneiro, J. V. Vidal, P. Rolo, I. Peres, J. A. F. Ferreira, A. L. Kholkin, M. P. Soares dos Santos, Instrumented electromagnetic generator: Optimized performance by automatic self-adaptation of the generator structure, *Mechanical Systems and Signal Processing*, 2022, **171**, 108898, doi: 10.1016/j.ymssp.2022.108898.
[29] H. Sharghi, O. Bilgen, Energy Harvesting from Human Walking Motion using Pendulum-based Electromagnetic Generators, *Journal of Sound and Vibration*, 2022, **534**, 117036, doi: 10.1016/j.jsv.2022.117036.
[30] K. Moradian, T. F. Sheikholeslami, M. Raghebi, Investigation of a spherical pendulum electromagnetic generator for harvesting energy from environmental vibrations and optimization using response surface methodology, *Energy Conversion and Management*, 2022, **266**, 115824, doi: 10.1016/j.enconman.2022.115824.
[31] Y. Xu, M. Ai, Z. Xu, Influence of partial winding fault on electromagnetic performance of permanent magnet wind generator with double three-phase winding, *Energy Reports*, 2021, **7**, 6462-6472, doi: 10.1016/j.egyr.2021.09.102.
[32] N. Savosteenko, N. Maksimov, I. Kiyessh, V. Kushnarev, Development of a Differential Electric Drive of a Starter-Generator based on a DC Motor, 2020 Russian Workshop on Power Engineering and Automation of Metallurgy Industry: Research & Practice (PEAMI), Magnitogorsk, Russia. IEEE, 2022.
[33] G. Milev, V. Gyurov, G. Ivanova, M. Duganov, B. Tzvetanov, Modelling and simulation of ships electric power station with self-excited brushless synchronous generators, 2021 13th Electrical Engineering Faculty Conference (BulEF). Varna, Bulgaria. IEEE, 2021.
[34] S. S. Kumar, S. Vignesh, R. Swathi, S. S. Saravanakumar, P. Vimal, Design and implementation of solar powered battery and diesel generator of electric vehicle charging station using hybrid intelligent controller, 2023 9th International Conference on Electrical Energy Systems (ICEES). Chennai, India. IEEE, 2023.
[35] L. L. Amuhaya, N. M. Muchuka, U. B. Akuru, M. J. Kamper, E. S. Obe, Permanent magnet wind generator with double excitation for smart grids, 2023 5th International Youth Conference on Radio Electronics, Electrical and Power Engineering (REEPE). Moscow, Russian Federation. IEEE, 2023.
[36] W. Ullah, F. Khan, U. B. Akuru, S. Hussain, M. Yousuf, S. Akbar, A novel dual electrical and dual mechanical wound field flux switching generator for co-rotating and counter-rotating wind turbine applications, *IEEE Transactions on Industry Applications*, 2024, **60**, 184-195, doi: 10.1109/TIA.2023.3314591.
[37] X. Hu, H. Wu, S. Liu, S. Gong, Y. Du, X. Li, X. Lu, J. Qu, Fabrication of organic shape-stabilized phase change material and its energy storage applications, *Engineered Science*, 2022, 17, 1-27, doi: 10.30919/es8d474.
[38] P. Naphon, S. Wiriyasart, Investigation on performance analysis of a small solar electric generator, *Case Studies in Thermal Engineering*, 2021, **27**, 101224, doi: 10.1016/j.csite.2021.101224.